

# Application of Nitrilotriacetic Acid Modified Gold Electrode for Determination of Lead in Natural Waters with Differential Pulse Adsorptive Cathodic Stripping Voltammetry

Marina Palcic<sup>1</sup>, Stjepan Milardovic<sup>2,\*</sup>, Irena Kerekovic<sup>2</sup> and Zorana Grabaric<sup>1</sup>

<sup>1</sup>Department of Chemistry and Biochemistry, Faculty of Food Technology and Biotechnology, University of Zagreb, Pierottijeva 6, 10000 Zagreb, Croatia

<sup>2</sup>Department of General and Inorganic Chemistry, Faculty of Chemical Engineering and Technology, University of Zagreb, Marulicev trg 19, 10000 Zagreb, Croatia

\*E-mail: [stjepan.milardovic@fkit.hr](mailto:stjepan.milardovic@fkit.hr)

Received: 20 February 2014 / Accepted: 18 March 2014 / Published: 14 April 2014

---

A self assembled monolayer of cysteamine (CA) was prepared on the surface of gold disc electrode and further modified with nitrilotriacetic acid (NTA). Characterization of prepared Au/CA/NTA electrode was done with cyclic voltammetry and electrochemical impedance spectroscopy in the presence of potassium hexacyanoferrate(II)/(III). Thus prepared electrode was tested for determination of lead. The response of modified electrode to  $Pb^{2+}$  concentration was measured by differential pulse adsorptive cathodic stripping voltammetry. Under the optimized working conditions (accumulation time, pH of accumulation and stripping solutions) the dependence of the stripping peak current response on concentration of  $Pb^{2+}$  was linear in the range of 0.002 – 10  $\mu$ M with a correlation coefficient of 0.9839. The interference of  $Co^{2+}$ ,  $Ni^{2+}$ ,  $Mg^{2+}$ ,  $Mn^{2+}$  and  $Ca^{2+}$  was found to be significantly reduced for analyte preconcentration from borate buffer pH = 7.0. Lead determination in potable and thermal water samples confirmed practical application of prepared sensor.

---

**Keywords:** Gold electrode; Nitrilotriacetic acid; Self assembled monolayer; Lead determination; Cathodic stripping voltammetry

## 1. INTRODUCTION

Global industrialization initiated high exploitation of natural resources in search for fuel and metals that are necessary for industrial development. This leads to increased concentration of heavy metals in the environment. Because of its abundant use in fuel industry during the past century, lead is one of the pollutants widespread in soil, especially in vicinity of high traffic roads, which enabled its integration into the food chain. Once ingested, heavy metals are distributed by blood to bones and soft tissues where they tend to accumulate [1]. Toxicological effects of lead to organs that are involved in

excretion process, such as kidneys and liver, are ascribed to oxidative stress causing various degenerative changes in soft tissue [2]. Oxidative stress induced by lead accumulation also affects central neural system leading to cognitive and motoric defects, as well as neurobehavioral alteration [3]. In order to monitor lead concentration in environment and all steps of food production, sensitive and accurate method needs to be developed. Some of the most sensitive techniques for lead determination in environmental and biological samples are atomic absorption spectrometry, inductively coupled plasma–atomic emission spectrometry and inductively coupled plasma–mass spectrometry. The main disadvantage of these techniques is high cost of equipment [4]. Electrochemical techniques, such as stripping analysis, require much cheaper equipment and still allow detection of metal traces. Dropping mercury electrode can be used to detect metal concentrations as low as 0.1 µg/L [5]. As alternative to toxic mercury electrodes, various non-toxic materials such as screen printed carbon [6], gold [7] or bismuth [8] are widely used. Application of metal electrodes (most frequently gold) with functionalized surface is another alternative for lead determination by voltammetric methods, such as square wave voltammetry, with the limit of detection as low as 0.5 µg/L [9].

Modification of metal electrode (gold, silver, copper and platinum) by self assembled monolayers (SAMs) based on organic thiols has been extensively studied over the last 20 years, since Nuzzo and Allara [10,11] discovered that alkenthiolate SAMs can be prepared by adsorption from diluted solution. Thiol SAMs provide platform for design of a broad number of functionalized layers on metal surfaces and can be easily engineered with variety of desired properties [12]. Modified SAMs can thus be applied for sensor construction for recognition of biologically important molecules such as glucose [13,14], dopamine [15], endotoxins [16], proteins [17], antioxidants [18], cholesterol [19], vitamins [20] antibodies and antigens [21] and DNA [22]. SAMs containing different surface groups (-OH, -NH<sub>2</sub>, -COOH, -PO<sub>4</sub><sup>2-</sup>) are widely used for complexation of metal ions like Cu<sup>2+</sup> [9,23,24], UO<sub>2</sub><sup>2+</sup> [25], Zr<sup>4+</sup> [26], F<sup>-</sup> [27], Mg<sup>2+</sup>, Ca<sup>2+</sup>, Sr<sup>2+</sup> [28] and lanthanide(III) [29]. SAMs terminated with nitrilotriacetic acid complexed with Me<sup>2+</sup> are used for selective immobilization of His-tagged proteins [30].

The main purpose of this research was to prepare a sensor with cysteamine self-assembled monolayer on gold electrode (Au/CA) functionalized with nitrilotriacetic acid (Au/CA/NTA). Due to tendency of NTA to form tetravalent chelate with various transition metals in bulk, sensor was used to measure lead concentration in different water samples by differential pulse adsorptive cathodic stripping voltammetry (DPAdCSV). The sensor was characterised with cyclic voltammetry (CV) and electrochemical impedance spectroscopy (EIS), methods recently used to study SAMs modified electrodes, electron transfer kinetics and determination of inorganic and organic substances [9,25].

## 2. EXPERIMENTAL

### 2.1. Chemicals and solutions

Cysteamine (CA) was obtained from Fluka, *N*-hydroxysuccinimide (NHS), 1-ethyl-3-(3-dimethylaminopropyl)carbodiimide hydrochloride (EDC) and nitrilotriacetic acid disodium salt (NTA) were from Sigma-Aldrich. Disodium hydrogen phosphate dihydrate, sodium dihydrogen phosphate

hydrate, acetic acid, sodium acetate, sodium perchlorate, disodium tetraborate decahydrate, hydrochloric acid and sodium hydroxide used for preparation and adjusting pH values of 0.1 M solutions of phosphate, acetate and 0.01 M borate buffer were purchased from Kemika. Ethanol for CA preparation, potassium hexacyanoferrate(II) and lead(II) nitrate were purchased from Kemika, too. Perchloric acid for electrochemical polishing and potassium hexacyanoferrate(III) were from Merck. Disodium ethylenediaminetetraacetic acid salt (EDTA) obtained by Sigma was used to prepare solution for sensor regeneration. All chemicals were of analytical grade and all solutions were prepared with ultra pure water from Millipore-MilliQ system (USA).

## 2.2. Instrumentation

All electrochemical measurements were carried out in a three-electrode cell. Gold disc and platinum wire were used as working and counter electrode, respectively. Reference electrode for CV and EIS measurements was Hg|Hg<sub>2</sub>Cl<sub>2</sub>|KCl saturated electrode (SCE) and for DPAdCSV measurements Ag|AgCl|3 M KCl. Solutions were deaerated with nitrogen for 10 min before measurements. All experiments were performed at room temperature.

Potentiostat 263 A (Princeton Applied Research, USA) connected to a computer for data collecting and analysis using EG&G-PowerSuite software was used for CV. All measurements were carried out at 50 mV/s scan rate.

The same potentiostat connected to frequency response detector model 1025 (PAR, USA), was used for EIS. The frequency range for impedance measurements was between 100 mHz and 100 kHz. Small sinusoidal AC signal of  $\pm 5$  mV was applied to +200 mV vs. SCE, formal potential of redox couple [Fe(CN)<sub>6</sub>]<sup>3-/4-</sup>. Equivalent circuit parameters were calculated by fitting the EIS data using appropriate circuit by EG&G ZsimpWin software.

Differential pulse adsorptive cathodic stripping voltammetry measurements were carried out on EG&G Princeton Applied Research (USA) Polarographic analyzer/stripping voltammeter Model 264 connected to computer via eDAQ e-corder model ED410 (Australia) for recording and analysis of experimental data. All stripping measurements were taken at 20 mV/s scan rate with 25 mV pulse amplitude.

ICP-MS Elan DRC (Perkin Elmer, USA) was used to analyse mineral content in thermal and spring waters.

## 2.3. Au/CA/NTA electrode preparation

A gold electrode of 1 mm diameter was chemically cleaned by 3 min immersion in Piranha solution (V(H<sub>2</sub>O<sub>2</sub>, 30 %):V(H<sub>2</sub>SO<sub>4</sub>, conc.) = 1:3), then polished on a flat pad to obtain mirror-like surface with SiC powder of different mesh (240, 800 and 1200) and finally by 1 and 0.25  $\mu$ m Al<sub>2</sub>O<sub>3</sub> powder. After electrode surface treatment with each polishing powder, electrode was ultrasonically cleaned in ultra pure water for 5 min followed by another 5 min in ethanol. Prior to next cleaning step, electrode was rinsed with ultra pure water. Subsequently, the Au electrode was electrochemically

polished in 0.1 M HClO<sub>4</sub> between 0 and 1.5 V until the stable cyclic voltammogram was obtained. Assuming 482 μC cm<sup>-2</sup> charge density for reduction of AuO monolayer, real electrode surface was calculated from the integration of reduction peak at 0.9 V vs. reference electrode, [31]. A roughness factor calculated as the ratio of real and geometric surface was 1.4.

Formation of CA self assembled monolayer, performed by immersion of electrode in 18 mM ethanolic solution of CA, was the first step in modification of a gold electrode. After approximately 24 h in dark at room temperature, electrode was removed from CA solution and thoroughly rinsed with ethanol to eliminate physically adsorbed species. For final modification EDC+NHS+NTA solution was prepared by mixing 2.9 mg NHS, 1.9 mg EDC and 11.8 mg NTA in 5 mL of 0.1 M phosphate buffer, pH = 5.0, and kept in darkness for 3 h to activate carboxyl group of NTA. Au/CA electrode was immersed in thus prepared solution for 24 h to covalently bind NTA to CA surface, resulting in Au/CA/NTA modified electrode. Possible way of coupling NTA to Au/CA surface is demonstrated in Fig. 1.

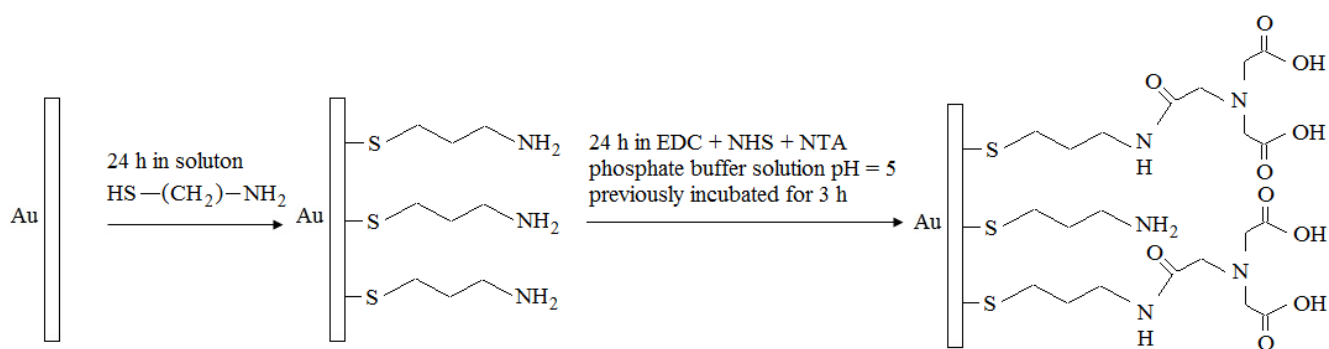


**Figure 1.** Functionalization of gold electrode with NTA through self assembled monolayer of cysteamine.

### 3. RESULTS AND DISCUSSION

#### 3.1. Characterization of Au/CA/NTA electrode

Generally, a self assembled structure created on the electrode forms layer that separates electrode surface from the solution bulk. That impedes electron transfer reactions causing increase in peak-to-peak separation ( $\Delta E_p$ ) and a decrease in both peak current ( $I_p$ ) and apparent rate constant of redox reaction [32]. Additionally, due to increase of functional groups subject to acid-base reactions, changes in environmental conditions (*e.g.* pH) can influence SAM's behavior to a great extent [33]. Since monolayers do not represent dense barrier between species in solution and electrode surface, this effect will be predominant in current and impedance response of SAM modified electrodes. In solutions containing  $[\text{Fe}(\text{CN})_6]^{3-/4-}$ , a reversible redox couple, CV and EIS responses depend mostly on the level of electrostatic interactions between negatively charged redox couple and electrode surface. Cyclic voltammograms and EIS measurements of Au, Au/CA and Au/CA/NTA electrode were recorded in solutions of 0.1 M acetate buffer (pH = 3.0) and 0.1 M phosphate buffer (pH = 9.0), both containing 0.1 M NaClO<sub>4</sub> and 1 M  $[\text{Fe}(\text{CN})_6]^{3-/4-}$ . Mathematical modelling of recorded impedance plots

was done using Randles equivalent circuit with constant phase element, CPE (Inset in Fig. 2b–C.) [34]. All parameter values presented in this work were calculated with respect to the unit electrode surface ( $1 \text{ cm}^2$ ).

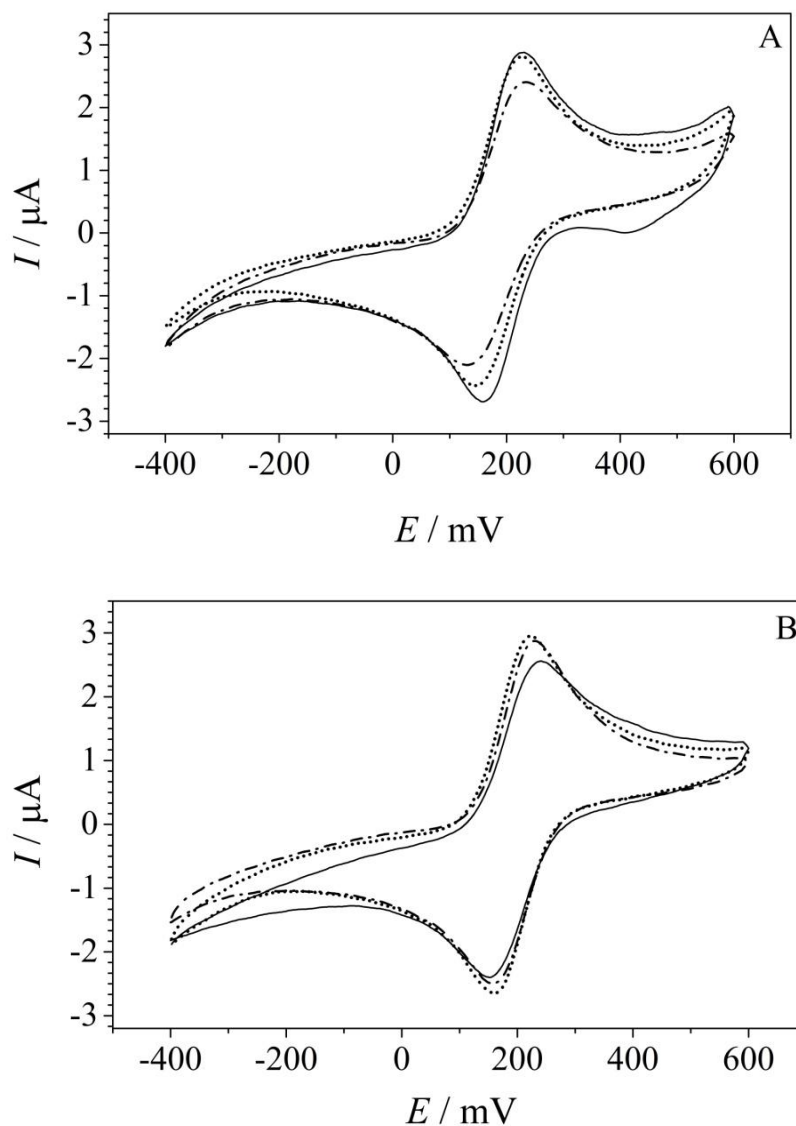


**Figure 2.** a) Cyclic voltammograms of Au (solid), Au/CA (dash) and Au/CA/NTA (dash-dot) electrodes in 0.1 M phosphate buffer pH = 9.0 (A) and in 0.1 M acetate buffer pH = 3.0 (B), both buffers containing 0.1 M  $\text{NaClO}_4$  and 1 mM  $[\text{Fe}(\text{CN})_6]^{3-/4-}$ .

### 3.1.1. Cyclic voltammetry

Cyclic voltammograms defined in alkaline and acidic buffers are presented in Fig. 2a. At pH = 9.0 (Fig. 2a–A.) amino group of cysteamine is not protonated, contributing to neutral surface charge of the electrode. Thus formed CA monolayer represents physical obstacle to direct contact between redox couple and Au electrode surface. Compared to bare gold electrode, slight decrease in  $I_p$ , an increase in  $\Delta E_p$  of approximately 10 mV, as well as absence of gold hydrous oxide reduction peak at 0.4 V [35] can be seen when electrode surface is covered with the first SAM. Further functionalization of surface

with NTA and formation of Au/CA/NTA SAM led to another decrease in  $I_p$  of approximately  $0.4 \mu\text{A}$  and increase in  $\Delta E_p$  of approximately  $20 \text{ mV}$ . Surface carboxyl groups of NTA are deprotonated at  $\text{pH} = 9.0$ , therefore electrostatic repulsion is blocking the approach of the negative redox couple to negatively charged electrode surface. In acidic solution *i.e.*  $\text{pH} = 3.0$  (Fig. 2a–B.) carboxyl and amino groups are highly protonated, resulting in different behavior of chemically modified electrode than in alkaline media. With protonated amino group of cysteamine, electrode surface is positively charged facilitating approach of a negative redox couple to electrode surface. It corresponds to increase of  $I_p$  ( $\sim 0.3 \mu\text{A}$ ) along with a decrease in  $\Delta E_p$  of  $\sim 30 \text{ mV}$  for Au/CA compared to unmodified electrode. Formation of peptide bond between NTA carboxyl and CA amino groups on the top of Au/CA electrode significantly decreased the number of free  $-\text{NH}_3^+$ , leading to decrease in  $I_p$  ( $\sim 0.2 \mu\text{A}$ ) and increase in  $\Delta E_p$ .

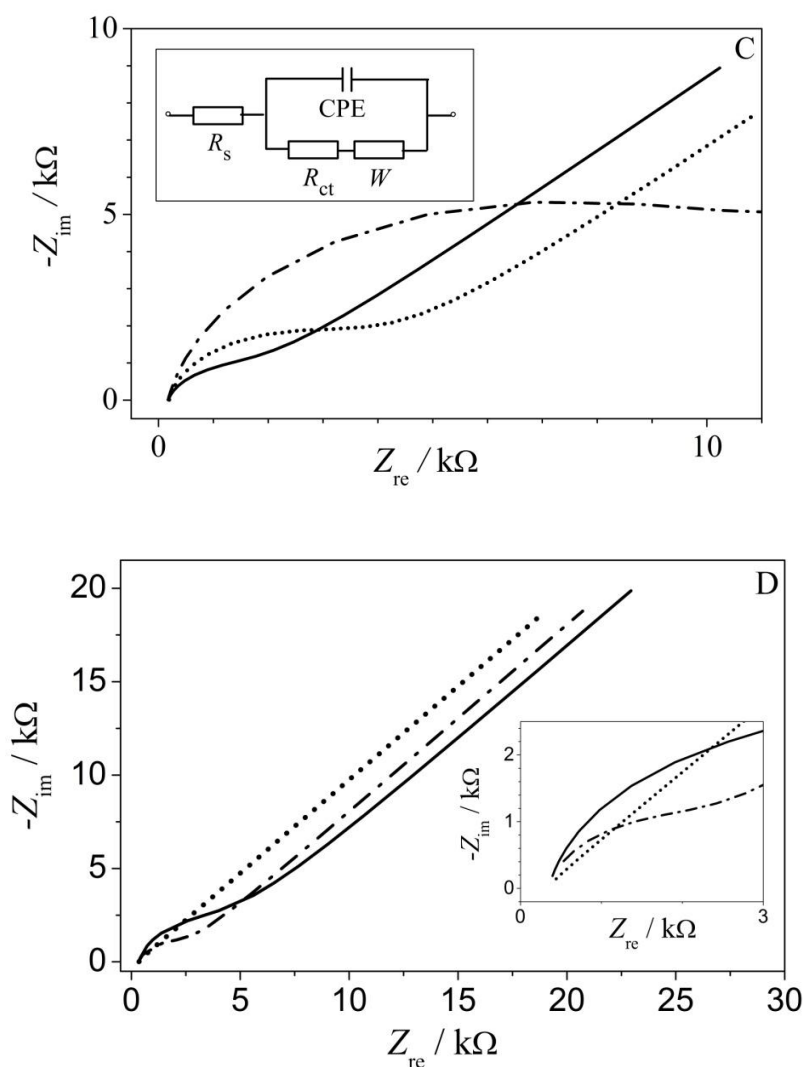


**Figure 2.** b) Nyquist plots of Au (solid), Au/CA (dash) and Au/CA/NTA (dash-dot) electrodes in 0.1 M phosphate buffer  $\text{pH} = 9.0$  (C) and 0.1 M acetate buffer  $\text{pH} = 3.0$  (D), both buffers containing 0.1 M  $\text{NaClO}_4$  and 1 mM  $[\text{Fe}(\text{CN})_6]^{3-/4-}$ . Inset (C) contains scheme of Randles equivalent circuit used for modeling of measured EIS data.

### 3.1.2. Electrochemical impedance spectroscopy

Generally, EIS results confirmed those obtained with CV. Binding of SAM on the electrode surface slows down electron transfer reactions, which is reflected in the increase of the charge transfer resistance *i.e.* enlargement of semicircular diameter. Formed CA monolayer, at pH = 9.0, demonstrated an increase in  $R_{ct}$  (Fig. 2b–C.) from 1.64 to 3.46 k $\Omega$ , correlating with decrease in  $I_p$  since amino group of cysteamine contributes to neutral surface charge at that pH. Further modification of surface with NTA monolayer led to another significant increase in  $R_{ct}$  to 11.02 k $\Omega$ , as a result of repulsion between negatively charged electrode surface and negative redox couple. As stated before, at acidic pH amino group of cysteamine is protonated, so electrode surface is positively charged, resulting in decrease (Fig. 2b–D) of  $R_{ct}$  from 3.88 to 0.79 k $\Omega$ . Formation of Au/CA/NTA led to increase in  $R_{ct}$  up to 1.71 k $\Omega$  as a consequence of adding another layer on top of Au/CA SAM. When comparing  $R_{ct}$  of Au/CA/NTA in acidic and alkaline media (about 6 times higher in alkaline), we can conclude that surface charge has much greater influence to apparent rate of redox reaction over thickness of barrier between redox couple in solution and Au surface. Influence of layer thickness is more evident in reduction of capacitance for measurements performed in both acidic and alkaline solutions, which is also in good agreement with the theory [36]. The values of  $n$  (surface roughness CPE parameter) changed from 0.85 to 0.89 in pH = 9.0 and 0.87 to 0.89 in pH = 3.0, indicating that SAM surface is "smoother" and behaviour of Au/CA/NTA electrode is more similar to an ideal capacitor than unmodified Au electrode [37]. Warburg impedance values are practically the same, *i.e.* the differences are negligible as expected if we assume that the thickness of the SAM is extremely small and does not affect the mass transfer of a redox couple from solution to the electrode surface.

### 3.2. Optimization of analytical conditions of Au/CA/NTA electrode

Lead determination in water samples is a two-step procedure. First step is adsorptive preconcentration of lead at open circuit potential onto Au/CA/NTA electrode from buffered sample solution. After that, cathodic differential pulse voltammograms are recorded from +600 to –400 mV in buffered  $Pb^{2+}$  free solutions. Between measurements, simple sensor regeneration is performed.

#### 3.2.1. Preconcentration of $Pb^{2+}$

Adsorption of  $Pb^{2+}$ , from continuously stirred solutions, onto Au/CA/NTA electrode performed at open circuit potential was optimized regarding duration of preconcentration step, as well as composition and pH of buffer solution. Duration of preconcentration step was studied and results are presented in Fig. 3. It can be seen that after 10 min of accumulation time signal is only slightly increasing (*i.e.* plateau was not reached). That is why 10 min was chosen as optimum preconcentration time for all further measurements.

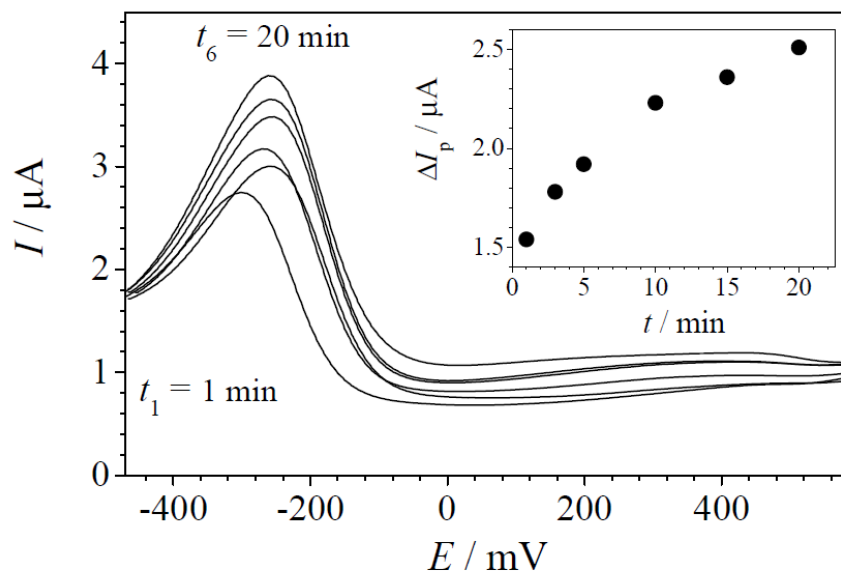


**Figure 3.** Cathodic stripping voltammograms of Au/CA/NTA electrode recorded in 0.01 M borate buffer pH = 8.0 at scan rate 20 mV/s, pulse height 25 mV after different accumulation time at pH = 7.0 (0.01 M borate buffer);  $c(\text{Pb}^{2+}) = 50 \mu\text{M}$ . Inset shows peak current of Au/CA/NTA electrode cathodic stripping voltammograms after different accumulation periods.

When evaluating the influence of chemical composition and pH of buffer solution on adsorption of Pb(II) species onto sensor surface, several parameters need to be assessed. Total negative surface charge, due to deprotonation of NTA at high pH, increases formation of complexes with cationic species, such as  $\text{Pb}^{2+}$  and  $\text{Pb}(\text{OH})^+$  [38]. Taking into consideration the surface  $pK$  value of NTA (6.6) bound to the electrode surface through one of the three carboxyl groups [39], it is expected that enhanced adsorption of  $\text{Pb}^{2+}$  should be achieved from solutions with pH values higher than 6.6. Similar work was presented by Shervedani et al. [9] where EDTA was used instead of NTA for complexation of metal ion on top of electrode surface from phosphate buffer solution. A significant signal decrease, as low as 20 % of maximum value (measured at pH = 3.0), was reported for pH = 7.0. The authors ascribed it to competition of  $\text{OH}^-$  (from accumulation solution) and EDTA (grafted on electrode surface) for binding of  $\text{Pb}^{2+}$ , disregarding at the same time the increasing influence of phosphate buffer as solution pH rises above 7. Taking into account solubility product of lead(II) hydroxide ( $pK_{\text{sp}} = 14.70$ ) [40], at micromolar concentrations of  $\text{Pb}^{2+}$  below pH 7 hydroxide will not precipitate. On the other hand when using 0.1 M phosphate buffer,  $\text{PbHPO}_4$  ( $pK_{\text{sp}} = 9.92$ ) [40] is expected to precipitate even from nanomolar solutions of  $\text{Pb}^{2+}$  as pH rises slightly above 7.0. In order to confirm previous statement, instead of phosphate buffer, accumulation was performed from acetate and borate buffer solutions at pH = 3.0 – 6.5 and 7.0 – 10.0, respectively. As shown in Fig. 4. no significant signal difference can be observed when preconcentration is performed in acetate buffer pH = 3.0 – 6.0. As pH approaches surface  $pK$  value of NTA, signal continues to increase with maximum at pH = 8.0. At high pH values (9 – 10) equilibrium concentration of hydroxide ions was at the point where precipitation of  $\text{Pb}(\text{OH})_2$  starts, which is obvious from the signal decrease. Borate buffer enables

determination of lead in alkaline solutions due to formation of stable lead-borate complex  $[\text{PbB}(\text{OH})_4]^+$  (formation constant  $\beta_1 = 5.21$ ) [41], *i.e.*  $\text{B}(\text{OH})_4^-$  competes with hydroxide ions in binding free  $\text{Pb}^{2+}$ . That is why, even in  $\text{pH} = 7.0 - 10.0$ , obtained signal values were two times higher than those obtained in acidic solutions. The other reason is higher deprotonation degree of NTA at higher  $\text{pH}$ , which enables greater electrostatic attraction of lead(II) cationic species to sensor surface. Results in Fig. 4. demonstrated that sigmoidal curve has inflection point at  $\text{pH} 6.5$  corresponding to NTA surface  $\text{p}K$  value. This confirms that hydroxide ions do not significantly influence formation of surface  $\text{NTA}^{2-}/\text{Pb}^{2+}$  complex at  $\text{pH}$  below 8, therefore  $0.01 \text{ mol L}^{-1}$ ,  $\text{pH} = 7.0$  borate buffer was chosen for further measurements.

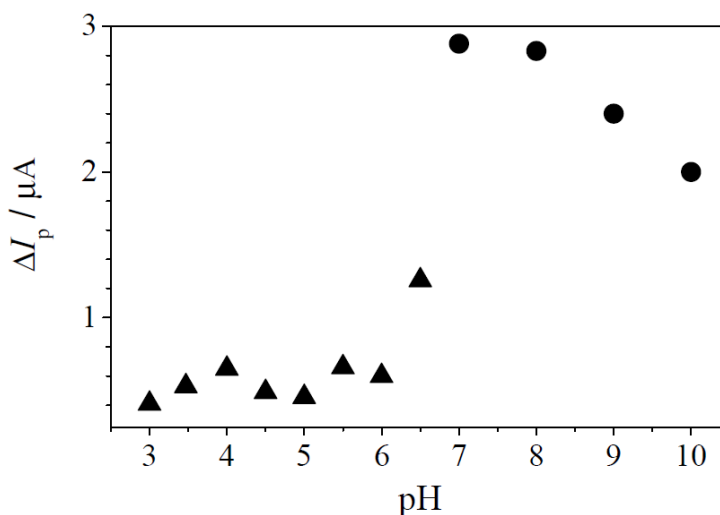


**Figure 4.** Peak current of Au/CA/NTA electrode cathodic stripping voltammogram after 10 min of adsorptive accumulation:  $c(\text{Pb}^{2+}) = 50 \mu\text{M}$ ;  $\text{pH} = 3.0 - 6.5$  (0.1 M acetate buffer, ▲);  $\text{pH} = 7.0 - 10.0$  (0.01 M borate buffer, ●). Stripping measurements were performed in 0.01 M borate buffer  $\text{pH} = 8.0$  at scan rate 20 mV/s, pulse height 25 mV.

### 3.2.2. Buffer composition and pH for stripping analysis

Main Optimization of stripping step implies that all parameters which influence desorption of metal from electrode surface have to be considered. Taking into account electrostatic nature of interaction between surface NTA and lead(II) cationic species, there are two pathways of desorption. One is to lower  $\text{pH}$  of stripping buffer leading to protonation of NTA carboxyl groups, and other is to facilitate depletion of lead from electrode surface by adding species that form more stable complexes or compounds of low solubility. Results presented in Fig. 5. show significantly lower signal values for measurements performed in solutions with  $\text{pH}$  below  $\text{p}K$  value of NTA (*i.e.* in acetate buffers), implying that lead(II) species are to a great extent desorbed before reduction step. For measurements performed in solutions with  $\text{pH}$  higher than  $\text{p}K$  value of NTA (*i.e.* in borate buffers,  $\text{pH} > 8$ )  $\Delta I_p$  are about two times higher than in acidic solutions. This indicates once again that equilibrium concentration of  $\text{OH}^-$  does not significantly contribute to desorption of lead(II) species via formation of  $\text{Pb}(\text{OH})_2$ . At the same time almost 50 % signal decrease is observed for measurements at  $\text{pH} = 8.0$

when 0.1 M phosphate buffer (dashed line) was used instead of 0.01 borate buffer, confirming higher influence of  $\text{HPO}_4^{2-}$  over  $\text{OH}^-$  equilibrium concentration on  $\text{Pb}^{2+}$  desorption. For stripping of lead(II), 0.01 M borate buffer pH = 8.0 was chosen as optimal.

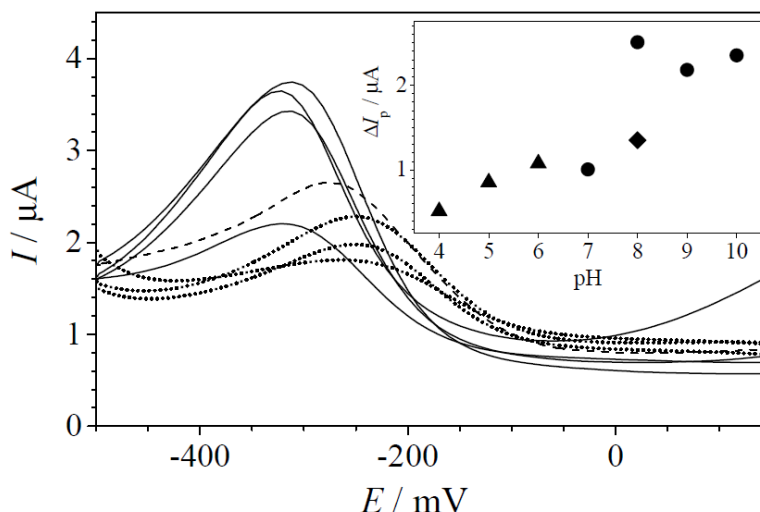


**Figure 5.** Cathodic stripping voltammogram of Au/CA/NTA electrode after 10 min of adsorptive accumulation: 0.01 M borate buffer pH = 7.0;  $c(\text{Pb}^{2+}) = 5.0 \mu\text{M}$ . Measurements were performed in: 0.1 M acetate buffer pH = 4.0 – 6.0 (dotted line); 0.01 M borate buffer pH = 7.0 – 10.0 (solid line) and 0.1 M phosphate buffer pH = 8.0 (dashed line) at scan rate 20 mV/s, pulse height 25 mV. Inset shows peak current for  $\text{Pb}^{2+}$  stripping performed in pH range 4.0 – 10.0 using acetate (▲), borate (●) and phosphate buffer (◆).  $\Delta I_p$  = peak current after background removal.

### 3.2.3. Sensor regeneration

Since lead was reduced on sensor surface during cathodic stripping analysis, it needed to be electrochemically oxidized for 30 s at +600 mV after each measurement. Only after that, two previously mentioned pathways of lead depletion from sensor surface can be used to regenerate sensor surface between measurements. One by immersion in perchloric acid pH = 1.0 – 3.0, or the other by chelating lead with ligand such as EDTA which forms more stable complexes than NTA ( $\log \beta_1(\text{NTA}) = 11.39$ ;  $\log \beta_1(\text{EDTA}) = 18.04$  [40]). After 3 min soaking in stirred 50 mM EDTA solution, preceded by applying potential of +600 mV for 30 s, lead free sensor surface was obtained. The efficiency of cleaning was confirmed by equalize the base current before metal accumulation and after treatment in EDTA cleaning solution.

### 3.2.4. Calibration

Response of Au/CA/NTA electrode, after 10 min electroless accumulation of  $\text{Pb}^{2+}$  from 0.01 M borate buffer pH = 7, was tested in the concentration range 0.001 – 100  $\mu\text{M}$  of  $\text{Pb}^{2+}$ , as presented in Fig. 6. Approximately four orders of magnitude linear range (0.002 – 10  $\mu\text{M}$ ) can, to some extent, be shifted towards lower detection limit by prolonging period of preconcentration. In that way, DPAdCSV can

compete in analysis of trace metals with other stripping methods where electrolysis is used to preconcentrate the target analyte on work electrode.

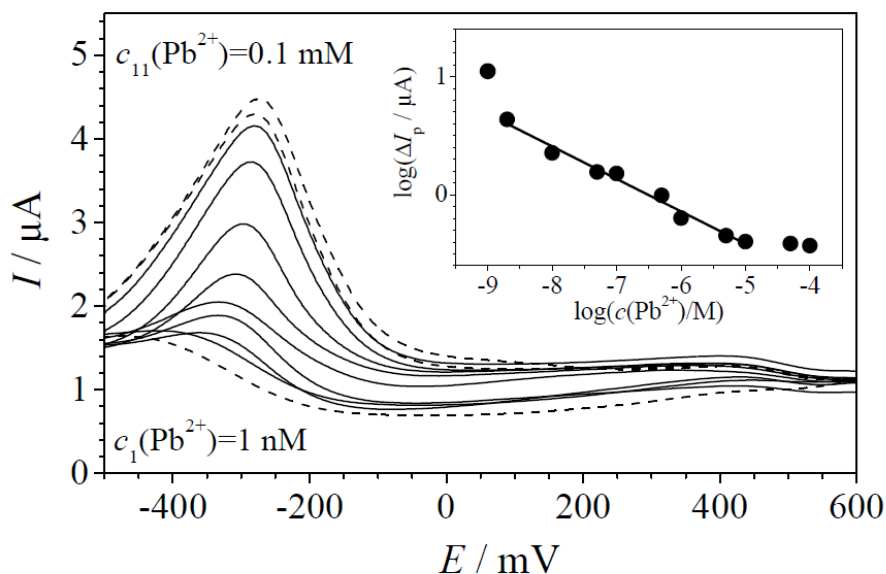


**Figure 6.** Response of Au/CA/NTA electrode after 10 min accumulation and stripping of  $Pb^{2+}$  from 0.01 M borate buffer pH = 7.0 and 8.0, respectively, at scan rate 20 mV/s and pulse height 25 mV. Inset shows electrode response which is linear for  $c(Pb^{2+}) = 0.002 - 10 \mu M$  defined with linear regression equation:  $\log(\Delta I_p/\mu A) = (1.77 \pm 0.09) + (0.27 \pm 0.01) \cdot \log(c(Pb^{2+})/M)$ ,  $R^2 = 0.9839$ .  $\Delta I_p$  = peak current after background removal.

### 3.2.5. Interferences

Influence of other cations on determination of lead in molar ratio  $c(Pb^{2+}):c(Me^{2+}) = 1:100$  is presented in Table 1.

**Table 1.** Effects of various metal ions on Au/CA/NTA electrode response to  $Pb^{2+}$  after 10 minute accumulation from 0.01 M borate buffer pH = 7 containing  $c(Pb^{2+}) = 50 \mu M$  and hundredfold more of tested interferente. Cathodic stripping voltammograms are recorded in 0.01 M borate buffer pH = 8 at scan rate 20 mV/s, pulse height 25 mV.

Interferente	$\Delta I_p(\text{interferente}+Pb^{2+})/\Delta I_p(Pb^{2+})$
$Cu^{2+}$	0.715
$Ni^{2+}$	0.771
$Co^{2+}$	0.782
$Mn^{2+}$	0.917
$Mg^{2+}$	0.903
$Ca^{2+}$	1.086
$Pb^{2+}$	1.000

As formation constants of complexes that various cations form with NTA change in the following sequence  $Mg^{2+} < Ca^{2+} < Mn^{2+} < Co^{2+} < Ni^{2+} < Pb^{2+} < Cu^{2+}$  [41], it is expected that metals forming less stable complexes with NTA in solution exhibit the same behavior when surface complexes are formed. Therefore, higher complex stability constant are expected to exhibit higher degree of interference. Results presented in Table 1. are in a good agreement with the previous statement.

### 3.2.6. Analytical application

**Table 2.** Results obtained from  $Pb^{2+}$  determination in synthetic samples and various samples of water diluted 1:10 with 0.01 M borate buffer pH = 7 and additionally spiked with  $Pb(NO_3)_2$  using Au/CA/NTA modified electrode.

Sample	$c(\text{added}) / \text{nmol L}^{-1}$	$c(\text{found}) / \text{nM}$	recovery / %
miliQ water2	50	$55.2 \pm 1.6$	110.4
miliQ water1	100	$103.1 \pm 3.3$	103.1
well spring ZG	100	$81.7 \pm 3.1$	81.7
well spring OS	100	$85.6 \pm 2.7$	85.6
thermal water	100	$77.1 \pm 4.0$	77.1

Note: Results are given as mean of 3 measurements  $\pm$  standard deviation.

Prior to determination of lead in various water samples using Au/CA/NTA electrode, ICP-MS was used to determine mineral content and assess level of interferents in tested samples. Prepared Au/CA/NTA electrode was then used to measure concentration of  $Pb^{2+}$  in different water samples spiked with known concentration of  $Pb(NO_3)_2$ . Results presented in Table 2 show good recovery for water samples when no interferents are present. About ~20 % lower recovery, at nanomolar level, was obtained for wellspring and thermal waters, which is satisfactory because of the high concentration of different interferents present in the samples. When analyzing Zagreb wellspring water containing 0.39 g/L of carbonates, measured value of  $Pb^{2+}$  is expected to be lower than added. Solubility product constant of lead(II) carbonate ( $pK_{sp}$  13.3) indicates that equilibrium concentration of free  $Pb^{2+}$  is decreased via formation of lead(II) carbonate [40]. Measured  $Pb^{2+}$  values in thermal water were lower than added, as well. This was attributed to high content of  $Mn^{2+}$ ,  $Cu^{2+}$  and  $Fe^{2+}$ , whose concentration exceeds that of  $Pb^{2+}$  by 100 to 10000 times, competing directly in adsorption onto sensor surface.

## 4. CONCLUSIONS

Modifying gold electrode with NTA via cysteamine SAM resulted in preparation of sensor surface exhibiting high affinity for binding lead. Sensor response was linear in a wide range of tested concentration (0.002 – 10  $\mu\text{M}$ ) which makes it suitable replacement for ecologically unacceptable mercury drop electrodes in determination of trace levels of lead. Electroless preconcentration of

lead(II) from borate buffer pH = 7.0 resulted in much higher voltammetric response compared to preconcentration from acidic solutions. Borate buffer enabled analysis of Pb<sup>2+</sup> to be performed at pH > 7 due to formation of stable but soluble lead-borate complex, thus preventing the precipitation of Pb(OH)<sub>2</sub>. Nanomolar concentrations of lead were determined with acceptable recovery in various water samples in spite of high levels of interferents (lead complexing species and metal cations) present.

#### ACKNOWLEDGEMENTS

We are grateful to the Croatian Ministry of Science, Education and Sports for the financial support of projects 058-0580000-3071 and 125-0000000-3210.

#### References

1. E.J. O'Flaherty, *Crit. Rev. Toxicol.*, 28 (1998) 271
2. G. Zheng, L. Tian, Y. Liang, K. Broberg, L. Lei, W. Guo, J. Nilsson, I.A. Bergdahl, S. Skerfving, T. Jin, *Neurotoxicology*, 32 (2011) 374
3. P. Reckziegel, V.T. Dias, D. Benvegnú, N. Boufleur, R.C. Silva Barcelos, H.J. Segat, C.S. Pase, C.M.M. dos Santos, T.M.M. Flores, M.E. Bürger, *Toxicol. Lett.*, 203 (2011) 74
4. E.P. Popek, *Sampling and analysis of environmental chemical pollutants: a complete guide*, Academic Press, San Diego, (2003)
5. P. Apostoli, *J. Chromatogr. B*, 778 (2002) 63.
6. K.C. Honeychurch, J.P. Hart, D.C. Cowell, D.W.M. Arrigan, *Sensor. Actuat. B-Chem.*, 77 (2001) 642
7. V. Beni, H.V. Newton, D.M.W. Arrigan, *Anal. Chim. Acta*, 502 (2004) 195
8. R. Kadara, I.E. Tothill, *Talanta*, 66 (2005) 1089
9. R.K. Shervedani, A. Farahbakhsh, M. Bagherzadeh, *Anal. Chim. Acta*, 587 (2007) 254
10. R.G. Nuzzo, D.L. Allara, *J. Am. Chem. Soc.*, 105 (1983) 4481
11. H.O. Finklea, *Self-assembled monolayers on electrodes. Encyclopedia of Analytical Chemistry, Applications, Theory and Instrumentation, Vol. 11*, Wiley, Chichester (2000)
12. A. Ulman, *Chem. Rev.*, 96 (1996) 1533
13. E.J. Calvo, R. Etchenique, L. Pietrasanta, A. Wolosiuk, C. Danilowicz, *Anal. Chem.*, 73 (2001) 1161
14. V. Anandan, R. Gangadharan, G.G. Zhang, *Sensors*, 9 (2009) 1295
15. Q. Wang, D. Dong, N.Q. Li, *Bioelectrochemistry*, 54 (2001) 169
16. S.J. Ding, B.W. Chang, C.C. Wu, C.J. Chen, H.C. Chang, *Electrochem. Commun.*, 9 (2007) 1206
17. K. Wadu-Mesthrige, N.A. Amro, G.Y. Liu, *Scanning*, 22 (2000) 380
18. S. Ignatov, D. Shishniashvili, B. Ge, F.W. Scheller, F. Lisdat, *Biosens. Bioelectron.*, 191 (2002) 17
19. T. Nakaminami, S. Ito, S. Kuwabata, H. Yoneyama, *Anal. Chem.*, 71 (1999) 1068
20. M.S. Alaejos, F.J.G. Montelongo, *Chem. Rev.*, 104 (2004) 3239
21. E. Katz, I. Willner, *J. Electroanal. Chem.*, 418 (1996) 67
22. F. Caruso, E. Rodda, D.F. Furlong, K. Niikura, Y. Okahata, *Anal. Chem.*, 69 (1997) 2043
23. F. Mirkhalaf, D.J. Schiffrin, *J. Chem. Soc.-Faraday Trans.*, 94 (1998) 1321
24. C. Fang, X.Y. Zhou, *Electroanal.*, 15 (2003) 1632
25. R.K. Shervedani, S.A. Mozaffari, *Surf. Coat. Technol.*, 198 (2005) 123
26. R.K. Shervedani, M. Bagherzadeh, *Electrochim. Acta*, 53 (2008) 6293
27. S. Zhang, C.M. Cardona, L. Echegoyen, *Chem. Commun.*, 43 (2006) 4461
28. D. Burshtain, D. Mandler, *Phys. Chem. Chem. Phys.*, 8 (2006) 158

29. M. Aihara, F. Tanaka, Y. Miyazaki, K. Takehara, *Anal. Lett.*, 35 (2002) 759
30. G.B. Sigal, C. Bamdad, A. Barberis, J. Strominger, G.M. Whitesides, *Anal. Chem.*, 68 (1996) 490
31. U. Oesch, J. Janata, *Electrochim. Acta*, 28 (1983) 1237
32. E. Sabatani, I. Rubinstein, R. Maoz, J. Sagiv, *J. Electroanal. Chem.*, 219 (1987) 365
33. C. Saby, B. Ortiz, G.Y. Champagne, D. Bélanger, *Langmuir*, 13 (1997) 6805
34. J.R. Macdonald, W.B. Johnson, *Fundamentals of impedance spectroscopy, 2nd ed. Vol. 2*, John Wiley & Sons Inc., New Jersey (2005)
35. J.D. Burke, J.M. Moran, P.F. Nugent, *J. Solid State Electrochem.*, 7 (2003) 529
36. E. Katz, I. Willner, *Electroanal.*, 15 (2003) 913
37. C.M.A. Brett, S. Kresak, T. Hianik, A.M. Oliviera-Brett, *Electroanal.*, 15 (2003) 557
38. K. J. Powell, P. L. Brown, R. H. Byrne, T. Gajda, G. Hefter, A.-K. Leuz, S. Sjöberg, H. Wanner, *Pure Appl. Chem.*, 81 (2009) 2425
39. T. Stora, R. Hovius, Z. Dienes, M. Pachoud, H. Vogel, *Langmuir*, 13 (1997) 5211
40. N. A. Lange, *Lange's handbook of chemistry, 15th ed.*, McGraw-Hill Inc., New York (1999)
41. S. Kotrlý, L. Šůcha, *Handbook of chemical equilibria in analytical chemistry*, John Wiley and sons, New York (1985)

© 2014 The Authors. Published by ESG ([www.electrochemsci.org](http://www.electrochemsci.org)). This article is an open access article distributed under the terms and conditions of the Creative Commons Attribution license (<http://creativecommons.org/licenses/by/4.0/>).